

Supplementary Information

Rate-determining step in the self-assembly process of supramolecular coordination capsules

Yuya Tsujimoto, Tatsuo Kojima and Shuichi Hiraoka*

Department of Basic Science, Graduate School of Arts and Sciences

The University of Tokyo

3-8-1 Komaba, Meguro-ku, Tokyo 153-8902, Japan

E-mail: chiraoka@mail.ecc.u-tokyo.ac.jp

Contents

- General information and materials S2
- Synthesis of tris-monodentate ligand **2** S2
- *n-k* Map for the assembly of an octahedron-shaped M_6L_8 molecular capsule (Fig. S1) S3
- General procedure for the investigation of the assembly process S4
- Determination of the average composition of the fragment species ($[Pd_aL_bPy_c]^{2a+}$) in each time point (Tables S1-21 and Figs S2 & S3) S4
- ESI-TOF mass study for the assembly of $[Pd_6L_8]^{12+}$ ($L = \mathbf{1}$ or **2**) capsules (Figs S4 and S5) S17
- The structural isomers of $[Pd_6L_8Py_2]^{12+}$ (Fig. S6) S19
- Molecular Mechanics investigation of the strain energy of the intermediates in the last step of the self-assembly process (Fig. S7 & Table S3) S19

General Information

¹H NMR and ¹³C NMR spectra were recorded with tetramethylsilane as the internal standard using a Bruker AV-500 (500 MHz) spectrometer. Electrospray ionization time-of-flight (ESI-TOF) mass spectra were obtained using a Waters Xevo G2 Tof mass spectrometer. Melting points were determined using a SCINICS SMP-300 instrument. Column chromatography was performed using SiO₂ [Merck, silica gel 60 for column chromatography (230-400 mesh ASTM)].

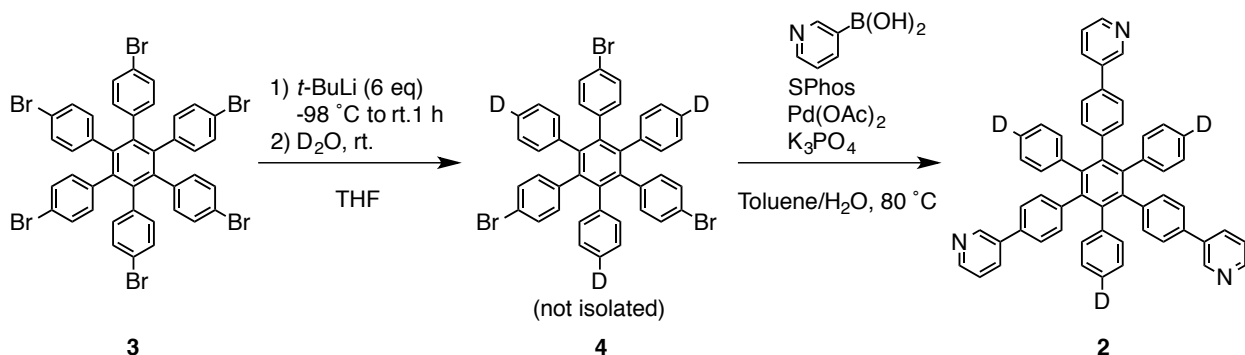
Materials

Unless otherwise noted, all solvents and reagents were obtained from commercial suppliers (TCI Co., Ltd., WAKO Pure Chemical Industries Ltd., KANTO Chemical Co., Ltd., and Sigma-Aldrich Co.) and were used as received.

Synthesis of tris-monodentate ligand **2**

Tris-monodentate ligand **2** was synthesized from **3**¹ in two steps (Scheme S1).

Scheme S1. Synthetic route of tris-monodentate ligand **2**



Synthesis of **4**²

To the suspension of **3** (1.00 g, 1.00 mmol) in THF (10 mL) was added a pentane solution of *t*-BuLi (6 eq) at -98 °C. After removal of the cooling bath, the reaction mixture was stirred for 1 h. Then the reaction was quenched by the addition of D₂O (3 mL) at room temperature. The mixture was partitioned between water and CHCl₃, and the aqueous layer was extracted with CHCl₃ (50 mL × 3). The combined extracts were dried over anhydrous MgSO₄ and the solvent was removed in vacuo to afford **4** (690 mg, 89%) as a colorless solid, which was used in the next step without further purification. ¹H NMR (500 MHz, CDCl₃, 298 K): δ 6.98 (dd, *J* = 6.6, 1.8 Hz, 6H), 6.91 (d, *J* = 8.1 Hz, 6H), 6.77 (d, *J* = 8.2 Hz, 6H), 6.66 (dd, *J* = 6.6, 1.8 Hz, 6H).

Synthesis of **2**

In a sealed flask, **4** (743 mg, 0.964 mmol), 2-dicyclohexylphosphino-2',6'-dimethoxybiphenyl (SPhos) (23.7 mg, 6 mol%), Pd(OAc)₂ (6.84 mg, 3 mol%), K₃PO₄ (1.23 g, 5.78 mmol), 3-pyridylboronic acid (533 mg, 4.34 mmol), H₂O (10 mL) and toluene (10 mL) were added. The mixture was stirred for 10 h at 90 °C. The mixture was partitioned between water and CH₂Cl₂, and the aqueous layer was extracted with CH₂Cl₂ (50 mL × 3). The combined extracts were dried over anhydrous MgSO₄ and the solvent was removed in vacuo. Silica-gel column chromatography (CHCl₃/MeOH = 100/1) afforded **2** (154 mg, 21%) as a colorless solid. m.p. >300 °C; ¹H NMR (500 MHz, CDCl₃, 298 K): δ 8.68 (d, *J* = 2.1 Hz, 3H), 8.49 (dd, *J* = 4.7, 1.5 Hz, 3H), 7.71 (dt, *J* = 8.0, 1.9 Hz, 3H), 7.25 (dd, *J* = 7.4, 4.8 Hz, 3H), 7.13 (d, *J* = 8.3 Hz, 6H), 6.95 (d, *J* = 8.3 Hz, 6H), 6.89 (s, 12H); ¹³C NMR (125 MHz, CDCl₃, 298 K): δ 148.25, 140.76, 140.72, 140.29, 140.06, 136.30, 134.47, 134.03, 132.27, 131.51, 126.94, 125.35, 123.46 (13 signals; One signal was not observed because of overlapping. The signal for the carbon attached to the deuterium was not observed because of negative NOE effects and splitting.); HRMS (ASAP): Calcd. for [M]⁺ C₅₇H₃₆D₃N₃ required 768.3379, found 768.3341.

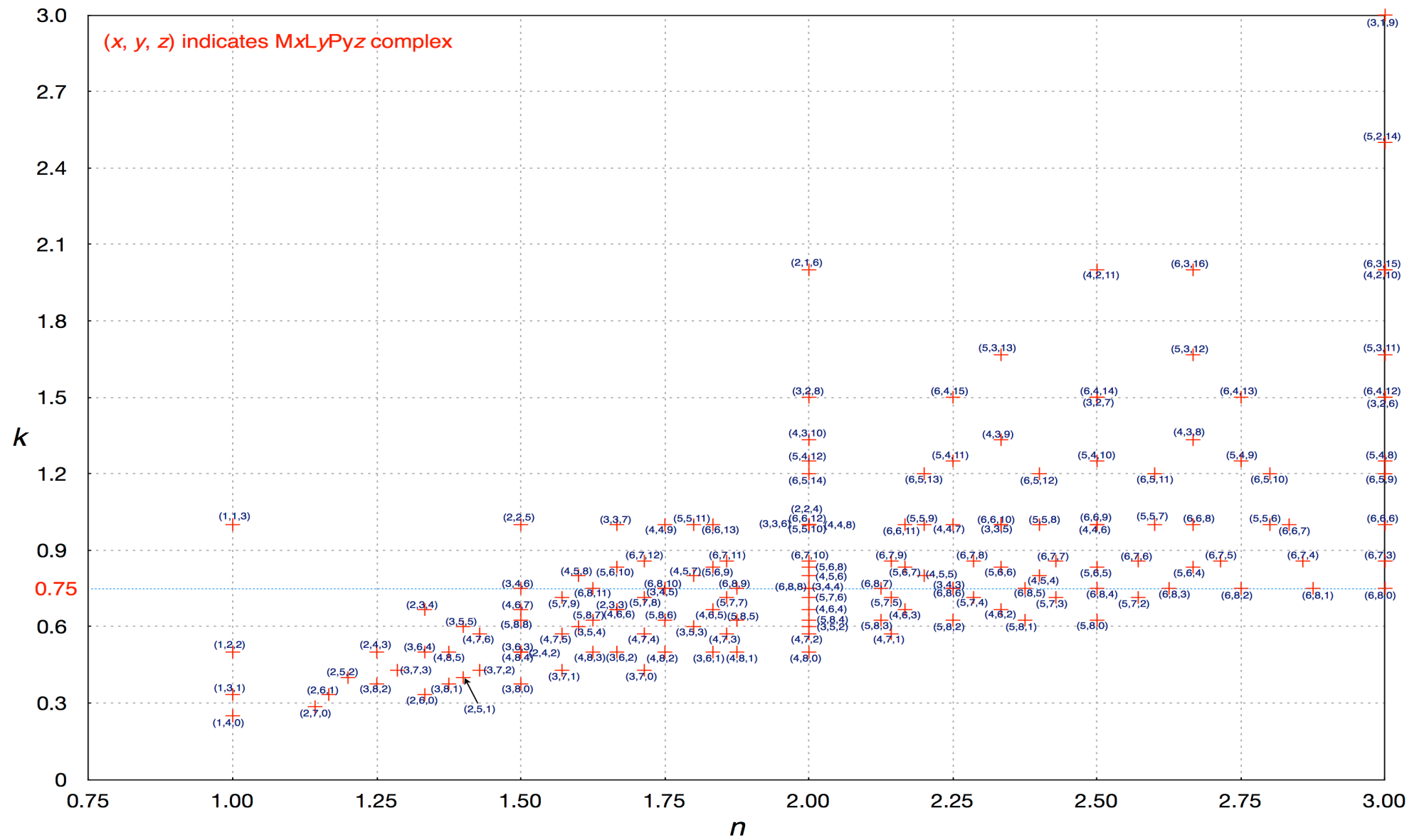


Fig. S1 n - k Map for the assembly of octahedron-shaped $M_6 L_8$ molecular capsules. The (n, k) values for species from $M_1 L_1 Py_3$ to $M_6 L_8$ (155 species) are plotted as crosshairs in red. The $M_x L_y P_y z$ complex is depicted as (x, y, z) .

General procedure for the investigation of the assembly process

To a NMR tube, panel molecule, **1**, (0.99 mg, 1.2 μmol), 1,3,5-trimethoxybenzene (0.05 mg, 0.3 mmol), CD₃CN (310 μL) and CD₂Cl₂ (100 μL) were added. The self-assembly was started by the addition of a solution of PdPy₄·(OTf)₂ (0.66 mg, 0.92 mmol) in CD₃CN (50 μL), and then the assembly process was monitored by ¹H NMR spectroscopy (500 MHz) with a 5-minute interval at 298 K. The quantities of **1**, [PdPy₄]²⁺, [Pd₆**1**₈]¹²⁺ and Py were quantified by the integral of each ¹H signal against the signal of the internal standard (1,3,5-trimethoxybenzene). The (*n*, *k*) values were obtained from the data thus obtained, and were plotted in the *n*-*k* map to obtain Fig. 2b. The quantities of **1**, [PdPy₄]²⁺, [Pd₆**1**₈]¹²⁺ and Py and the (*n*, *k*) values at each time are listed in Tables S2-S11. In order to evaluate the reproducibility and validity, the same experiment was repeated ten times (Fig. S2). The investigation of the self-assembly for [Pd₆**2**₈]¹²⁺ was carried out in the same way. Selected ¹H NMR spectra are shown in Fig. 3b. The (Pd_x**2**_yPy_z)_{ave} and (*n*, *k*) values at each time are listed and plotted in Tables S12-S21 and Fig. S3.

Determination of the average composition of the fragment species, [Pd_aL_bPy_c]^{2a+}, in each time point

The amounts of **L**, [Pd(Py)₄]²⁺, [Pd₆**L**₈]¹²⁺ and Py at each time point during the self-assembly process were quantified by ¹H NMR measurements in the presence of 1,3,5-trimethoxybenzene as an internal standard.

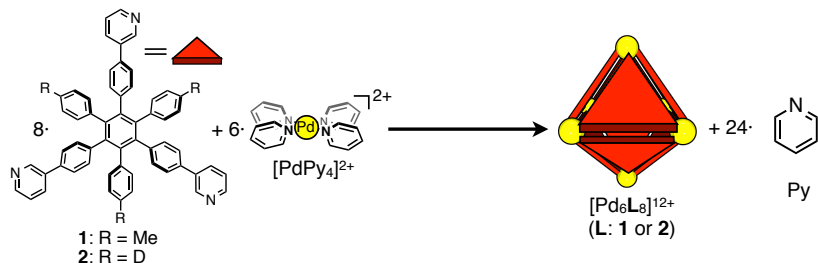


Table S1. The quantities of each component of the above scheme

Time	L	[PdPy ₄] ²⁺	[Pd ₆ L ₈] ¹²⁺	Py
0	<i>l</i> ₀	<i>m</i> ₀	0	0
<i>t</i>	<i>l</i> _{<i>t</i>}	<i>m</i> _{<i>t</i>}	<i>n</i> _{<i>t</i>}	<i>o</i> _{<i>t</i>}

At time *t*, the quantities of Pd²⁺ ion, panel molecule, **L** and Py in the average composition of the fragmentary species, (Pd_a**L**_bPy_c)_{ave}, are expressed by equations (3) – (5).

$$a = m_0 - m_t - 6 \cdot n_t \quad \dots \dots (3)$$

$$b = l_0 - l_t - 8 \cdot n_t \quad \dots \dots (4)$$

$$c = 4 \cdot m_0 - 4 \cdot m_t - o_t \quad \dots \dots (5)$$

where *l*₀ and *m*₀ are the quantities for **L** and [PdPy₄]²⁺, respectively at time = 0 and *l*_{*t*}, *m*_{*t*}, *n*_{*t*} and *o*_{*t*} are the quantities for **L**, [PdPy₄]²⁺, [Pd₆**L**₈]¹²⁺ and Py, respectively at time = *t* (Supplementary Table S1).

Then, the (*n*, *k*) values for (Pd_a**L**_bPy_c)_{ave} at each time point were determined by equations (1) and (2) in the main text. The date obtained by ten experiments for the self-assembly of [Pd₆**1**₈]¹²⁺ and [Pd₆**2**₈]¹²⁺ are listed in Tables S2-S11 and S12-S21, respectively.

Table S2. The quantities of **1**, $[\text{Pd}_6\mathbf{1}_8]^{12+}$, $[\text{PdPy}_4]^{2+}$ and Py and the (*n*, *k*) values at each time point for the assembly of $[\text{Pd}_6\mathbf{1}_8]^{12+}$ (1st run)

Time (min)	1 (μmol)	$[\text{Pd}_6\mathbf{1}_8]^{12+}$ (μmol)	$[\text{PdPy}_4]^{2+}$ (μmol)	Py (μmol)	<i>n</i>	<i>k</i>
0	1.170	0	0.878	0		
5	0.329	0.008	0.242	2.066	2.436	0.781
10	0.284	0.016	0.198	2.430	2.571	0.772
15	0.228	0.025	0.163	2.646	2.591	0.764
20	0.206	0.043	0.146	2.781	2.723	0.762
25	0.191	0.053	0.139	2.862	2.860	0.753
30	0.179	0.060	0.133	2.916	2.884	0.759
35	0.154	0.066	0.112	2.984	2.873	0.761
40	0.149	0.070	0.112	3.011	2.855	0.755
45	0.140	0.073	0.104	3.024	2.879	0.755
50	0.130	0.077	0.097	3.078	2.880	0.757
55	0.125	0.079	0.094	3.092	2.881	0.753
60	0.124	0.082	0.093	3.092	2.859	0.754
70	0.117	0.087	0.086	3.105	2.857	0.749
80	0.099	0.089	0.073	3.173	2.871	0.756
90	0.096	0.091	0.073	3.186	2.880	0.757
180	0.072	0.105	0.054	3.267	2.879	0.758
360	0.060	0.112	0.045	3.308	2.864	0.756

Table S3. The quantities of **1**, $[\text{Pd}_6\mathbf{1}_8]^{12+}$, $[\text{PdPy}_4]^{2+}$ and Py and the (*n*, *k*) values at each time point for the assembly of $[\text{Pd}_6\mathbf{1}_8]^{12+}$ (2nd run)

Time (min)	1 (μmol)	$[\text{Pd}_6\mathbf{1}_8]^{12+}$ (μmol)	$[\text{PdPy}_4]^{2+}$ (μmol)	Py (μmol)	<i>n</i>	<i>k</i>
0	1.125	0	0.847	0		
5	0.311	0.023	0.218	2.133	2.513	0.779
10	0.257	0.029	0.186	2.511	2.851	0.765
15	0.225	0.046	0.164	2.619	2.848	0.766
20	0.209	0.057	0.150	2.687	2.866	0.771
25	0.203	0.061	0.145	2.714	2.882	0.774
30	0.181	0.066	0.130	2.795	2.908	0.771
35	0.161	0.073	0.120	2.835	2.851	0.762
40	0.153	0.077	0.111	2.876	2.885	0.770
45	0.140	0.080	0.105	2.916	2.889	0.762
50	0.126	0.085	0.094	2.957	2.872	0.762
55	0.123	0.088	0.093	2.970	2.881	0.759
60	0.122	0.092	0.088	2.970	2.857	0.777
70	0.120	0.098	0.092	2.997	2.915	0.756
80	0.107	0.103	0.081	3.024	2.849	0.762
90	0.099	0.105	0.075	3.051	2.858	0.764

Table S4. The quantities of **1**, $[\text{Pd}_6\mathbf{1}_8]^{12+}$, $[\text{PdPy}_4]^{2+}$ and Py and the (*n*, *k*) values at each time point for the assembly of $[\text{Pd}_6\mathbf{1}_8]^{12+}$ (3rd run)

Time (min)	1 (μmol)	$[\text{Pd}_6\mathbf{1}_8]^{12+}$ (μmol)	$[\text{PdPy}_4]^{2+}$ (μmol)	Py (μmol)	<i>n</i>	<i>k</i>
0	1.134	0	0.851	0		
5	0.315	0.014	0.223	2.079	2.465	0.769
10	0.261	0.020	0.193	2.309	2.563	0.754
15	0.240	0.038	0.178	2.565	2.804	0.754
20	0.209	0.046	0.155	2.687	2.840	0.753
25	0.186	0.054	0.140	2.768	2.853	0.749
30	0.168	0.060	0.125	2.795	2.789	0.753
35	0.165	0.064	0.118	2.822	2.811	0.763
40	0.147	0.072	0.110	2.916	2.889	0.749
45	0.136	0.076	0.104	2.930	2.833	0.746
50	0.125	0.081	0.096	2.970	2.842	0.743
55	0.118	0.084	0.090	2.970	2.773	0.744
60	0.113	0.087	0.088	3.011	2.840	0.741
70	0.100	0.093	0.079	3.038	2.779	0.737
80	0.095	0.096	0.075	3.065	2.810	0.736
90	0.088	0.099	0.072	3.105	2.868	0.726

Table S5. The quantities of **1**, $[\text{Pd}_6\mathbf{1}_8]^{12+}$, $[\text{PdPy}_4]^{2+}$ and Py and the (*n*, *k*) values at each time point for the assembly of $[\text{Pd}_6\mathbf{1}_8]^{12+}$ (4th run)

Time (min)	1 (μmol)	$[\text{Pd}_6\mathbf{1}_8]^{12+}$ (μmol)	$[\text{PdPy}_4]^{2+}$ (μmol)	Py (μmol)	<i>n</i>	<i>k</i>
0	1.134	0	0.851	0		
5	0.323	0.012	0.230	2.039	2.450	0.767
10	0.268	0.017	0.198	2.471	2.826	0.755
15	0.229	0.040	0.167	2.619	2.835	0.757
20	0.203	0.053	0.148	2.741	2.893	0.757
25	0.167	0.060	0.127	2.822	2.838	0.747
30	0.161	0.066	0.120	2.862	2.873	0.751
35	0.153	0.070	0.114	2.903	2.905	0.752
40	0.147	0.073	0.109	2.916	2.885	0.753
45	0.126	0.078	0.095	2.970	2.859	0.748
50	0.122	0.082	0.093	2.984	2.849	0.744
55	0.113	0.086	0.087	3.011	2.845	0.743
60	0.114	0.089	0.090	3.011	2.843	0.737
70	0.111	0.092	0.084	3.038	2.887	0.748
80	0.099	0.095	0.076	3.065	2.851	0.744
90	0.099	0.098	0.076	3.078	2.894	0.742

Table S6. The quantities of **1**, $[\text{Pd}_6\mathbf{1}_8]^{12+}$, $[\text{PdPy}_4]^{2+}$ and Py and the (*n*, *k*) values at each time point for the assembly of $[\text{Pd}_6\mathbf{1}_8]^{12+}$ (5th run)

Time (min)	1 (μmol)	$[\text{Pd}_6\mathbf{1}_8]^{12+}$ (μmol)	$[\text{PdPy}_4]^{2+}$ (μmol)	Py (μmol)	<i>n</i>	<i>k</i>
0	1.161	0	0.874	0		
5	0.333	0.012	0.245	2.201	2.614	0.761
10	0.274	0.020	0.201	2.430	2.680	0.760
15	0.235	0.043	0.174	2.700	2.866	0.759
20	0.200	0.057	0.149	2.849	2.930	0.758
25	0.195	0.068	0.147	2.862	2.916	0.756
30	0.180	0.071	0.135	2.903	2.902	0.759
35	0.156	0.076	0.119	2.957	2.851	0.753
40	0.147	0.080	0.114	2.997	2.877	0.748
45	0.130	0.083	0.102	3.051	2.882	0.745
50	0.127	0.086	0.102	3.078	2.930	0.741
55	0.119	0.087	0.093	3.092	2.900	0.749
60	0.110	0.089	0.088	3.105	2.858	0.743
70	0.107	0.095	0.085	3.132	2.899	0.745
80	0.101	0.099	0.083	3.159	2.920	0.736
90	0.095	0.103	0.079	3.173	2.900	0.735

Table S7. The quantities of **1**, $[\text{Pd}_6\mathbf{1}_8]^{12+}$, $[\text{PdPy}_4]^{2+}$ and Py and the (*n*, *k*) values at each time point for the assembly of $[\text{Pd}_6\mathbf{1}_8]^{12+}$ (6th run)

Time (min)	1 (μmol)	$[\text{Pd}_6\mathbf{1}_8]^{12+}$ (μmol)	$[\text{PdPy}_4]^{2+}$ (μmol)	Py (μmol)	<i>n</i>	<i>k</i>
0	1.152	0	0.861	0		
5	0.331	0.017	0.241	2.066	2.420	0.756
10	0.257	0.021	0.194	2.336	2.522	0.744
15	0.219	0.034	0.164	2.525	2.585	0.744
20	0.214	0.050	0.156	2.741	2.864	0.753
25	0.185	0.060	0.137	2.849	2.889	0.747
30	0.172	0.065	0.129	2.876	2.858	0.742
35	0.154	0.069	0.117	2.916	2.825	0.739
40	0.154	0.073	0.110	2.916	2.812	0.754
45	0.140	0.078	0.104	2.957	2.791	0.743
50	0.130	0.081	0.098	2.997	2.811	0.738
55	0.123	0.084	0.095	3.024	2.827	0.735
60	0.124	0.088	0.095	3.024	2.815	0.735
70	0.113	0.094	0.086	3.065	2.811	0.732
80	0.105	0.097	0.079	3.105	2.872	0.738
90	0.104	0.100	0.079	3.105	2.839	0.731

Table S8. The quantities of **1**, $[Pd_6\mathbf{1}_8]^{12+}$, $[PdPy_4]^{2+}$ and Py and the (*n*, *k*) values at each time point for the assembly of $[Pd_6\mathbf{1}_8]^{12+}$ (7th run)

Time (min)	1 (μmol)	$[Pd_6\mathbf{1}_8]^{12+}$ (μmol)	$[PdPy_4]^{2+}$ (μmol)	Py (μmol)	<i>n</i>	<i>k</i>
0	1.143	0	0.854	0		
5	0.320	0.014	0.209	1.917	2.224	0.790
10	0.274	0.023	0.192	2.336	2.603	0.765
15	0.262	0.046	0.189	2.525	2.770	0.757
20	0.232	0.051	0.170	2.660	2.854	0.751
25	0.214	0.056	0.158	2.727	2.876	0.749
30	0.185	0.061	0.136	2.822	2.885	0.748
35	0.161	0.065	0.119	2.889	2.876	0.746
40	0.144	0.069	0.110	2.943	2.878	0.738
45	0.148	0.075	0.107	2.943	2.891	0.752
50	0.138	0.079	0.102	2.970	2.878	0.744
55	0.126	0.084	0.096	3.011	2.884	0.737
60	0.118	0.086	0.089	3.038	2.887	0.737
70	0.112	0.089	0.084	3.065	2.907	0.739
80	0.104	0.094	0.079	3.078	2.858	0.733
90	0.099	0.095	0.075	3.092	2.859	0.735

Table S9. The quantities of **1**, $[Pd_6\mathbf{1}_8]^{12+}$, $[PdPy_4]^{2+}$ and Py and the (*n*, *k*) values at each time point for the assembly of $[Pd_6\mathbf{1}_8]^{12+}$ (8th run)

Time (min)	1 (μmol)	$[Pd_6\mathbf{1}_8]^{12+}$ (μmol)	$[PdPy_4]^{2+}$ (μmol)	Py (μmol)	<i>n</i>	<i>k</i>
0	1.269	0	0.955	0		
5	0.358	0.010	0.243	2.282	2.456	0.785
10	0.283	0.021	0.195	2.700	2.684	0.775
15	0.229	0.051	0.165	2.930	2.699	0.765
20	0.194	0.062	0.144	3.105	2.794	0.758
25	0.167	0.072	0.127	3.213	2.825	0.755
30	0.158	0.079	0.115	3.267	2.859	0.763
35	0.146	0.086	0.107	3.294	2.826	0.764
40	0.128	0.092	0.095	3.375	2.881	0.762
45	0.125	0.092	0.090	3.389	2.893	0.767
50	0.113	0.096	0.083	3.402	2.828	0.763
55	0.108	0.099	0.079	3.443	2.890	0.766
60	0.104	0.101	0.078	3.443	2.856	0.761
70	0.095	0.105	0.072	3.483	2.887	0.758
80	0.087	0.109	0.065	3.497	2.843	0.763
90	0.080	0.115	0.063	3.537	2.887	0.749

Table S10. The quantities of **1**, $[\text{Pd}_6\mathbf{1}_8]^{12+}$, $[\text{PdPy}_4]^{2+}$ and Py and the (n, k) values at each time point for the assembly of $[\text{Pd}_6\mathbf{1}_8]^{12+}$ (9th run)

Time (min)	1 (μmol)	$[\text{Pd}_6\mathbf{1}_8]^{12+}$ (μmol)	$[\text{PdPy}_4]^{2+}$ (μmol)	Py (μmol)	<i>n</i>	<i>k</i>
0	1.143	0	0.861	0		
5	0.376	0.011	0.270	2.052	2.634	0.773
10	0.276	0.017	0.206	2.403	2.729	0.756
15	0.234	0.038	0.182	2.606	2.800	0.746
20	0.218	0.048	0.171	2.700	2.860	0.741
25	0.204	0.054	0.163	2.768	2.904	0.737
30	0.188	0.065	0.152	2.835	2.932	0.734
35	0.184	0.068	0.146	2.849	2.929	0.739
40	0.170	0.070	0.133	2.862	2.862	0.745
45	0.168	0.076	0.132	2.889	2.904	0.743
50	0.158	0.079	0.127	2.903	2.853	0.737
55	0.153	0.082	0.122	2.943	2.919	0.740
60	0.143	0.083	0.116	2.957	2.870	0.734
70	0.131	0.087	0.108	2.997	2.881	0.732
80	0.125	0.091	0.104	3.024	2.898	0.728
90	0.122	0.092	0.102	3.024	2.859	0.724

Table S11. The quantities of **1**, $[\text{Pd}_6\mathbf{1}_8]^{12+}$, $[\text{PdPy}_4]^{2+}$ and Py and the (n, k) values at each time point for the assembly of $[\text{Pd}_6\mathbf{1}_8]^{12+}$ (10th run)

Time (min)	1 (μmol)	$[\text{Pd}_6\mathbf{1}_8]^{12+}$ (μmol)	$[\text{PdPy}_4]^{2+}$ (μmol)	Py (μmol)	<i>n</i>	<i>k</i>
0	1.224	0	0.908	0		
5	0.370	0.010	0.244	2.079	2.374	0.78
10	0.290	0.018	0.194	2.417	2.514	0.766
15	0.255	0.042	0.176	2.687	2.651	0.759
20	0.230	0.051	0.161	2.876	2.815	0.751
25	0.203	0.061	0.136	2.984	2.854	0.762
30	0.180	0.066	0.121	3.065	2.869	0.757
35	0.167	0.073	0.116	3.105	2.863	0.748
40	0.158	0.078	0.107	3.146	2.885	0.754
45	0.151	0.082	0.099	3.159	2.858	0.761
50	0.145	0.085	0.093	3.186	2.871	0.764
55	0.137	0.090	0.087	3.213	2.869	0.765
60	0.127	0.093	0.083	3.254	2.894	0.756
70	0.113	0.097	0.074	3.294	2.879	0.752
80	0.111	0.102	0.071	3.308	2.891	0.757
90	0.099	0.104	0.062	3.335	2.861	0.756
180	0.080	0.114	0.045	3.402	2.867	0.768
360	0.069	0.123	0.041	3.443	2.876	0.758

Table S12. The quantities of **2**, $[\text{Pd}_6\mathbf{2}_8]^{12+}$, $[\text{PdPy}_4]^{2+}$ and Py and the (n, k) values at each time point for the assembly of $[\text{Pd}_6\mathbf{2}_8]^{12+}$ (1st run)

Time (min)	2 (μmol)	$[\text{Pd}_6\mathbf{2}_8]^{12+}$ (μmol)	$[\text{PdPy}_4]^{2+}$ (μmol)	Py (μmol)	n	k
0	1.278	0	0.952	0		
5	0.372	0	0.235	2.133	2.354	0.791
10	0.301	0.024	0.194	2.444	2.377	0.781
15	0.281	0.035	0.183	2.633	2.501	0.779
20	0.256	0.045	0.173	2.876	2.712	0.767
25	0.248	0.052	0.170	2.903	2.691	0.764
30	0.233	0.063	0.161	2.984	2.719	0.763
35	0.214	0.067	0.145	3.011	2.655	0.766
40	0.205	0.073	0.141	3.051	2.658	0.763
45	0.203	0.078	0.138	3.092	2.708	0.767
50	0.196	0.082	0.135	3.119	2.700	0.763
55	0.194	0.087	0.133	3.146	2.721	0.764
60	0.182	0.090	0.126	3.173	2.692	0.759
70	0.176	0.095	0.120	3.200	2.690	0.766
80	0.170	0.098	0.116	3.227	2.698	0.766
90	0.167	0.102	0.115	3.240	2.692	0.764
180	0.157	0.119	0.110	3.308	2.665	0.754
360	0.160	0.132	0.112	3.335	2.682	0.773

Table S13. The quantities of **2**, $[\text{Pd}_6\mathbf{2}_8]^{12+}$, $[\text{PdPy}_4]^{2+}$ and Py and the (n, k) values at each time point for the assembly of $[\text{Pd}_6\mathbf{2}_8]^{12+}$ (2nd run)

Time (min)	2 (μmol)	$[\text{Pd}_6\mathbf{2}_8]^{12+}$ (μmol)	$[\text{PdPy}_4]^{2+}$ (μmol)	Py (μmol)	n	k
0	1.278	0	0.955	0		
5	0.408	0	0.253	2.214	2.544	0.807
10	0.303	0.021	0.193	2.525	2.504	0.788
15	0.277	0.033	0.183	2.646	2.518	0.780
20	0.263	0.042	0.178	2.849	2.710	0.773
25	0.252	0.051	0.174	2.943	2.783	0.769
30	0.239	0.059	0.162	2.970	2.744	0.775
35	0.221	0.067	0.150	3.038	2.746	0.775
40	0.212	0.072	0.147	3.078	2.752	0.766
45	0.195	0.079	0.139	3.132	2.745	0.760
50	0.195	0.081	0.136	3.132	2.732	0.766
55	0.190	0.087	0.135	3.173	2.764	0.761
60	0.188	0.090	0.132	3.173	2.739	0.764
70	0.178	0.096	0.124	3.227	2.779	0.768
80	0.169	0.101	0.115	3.254	2.756	0.777
90	0.166	0.103	0.117	3.267	2.755	0.764
180	0.155	0.123	0.111	3.335	2.748	0.762
360	0.146	0.131	0.104	3.375	2.820	0.776

Table S14. The quantities of **2**, $[\text{Pd}_6\mathbf{2}_8]^{12+}$, $[\text{PdPy}_4]^{2+}$ and Py and the (n, k) values at each time point for the assembly of $[\text{Pd}_6\mathbf{2}_8]^{12+}$ (3rd run)

Time (min)	2 (μmol)	$[\text{Pd}_6\mathbf{2}_8]^{12+}$ (μmol)	$[\text{PdPy}_4]^{2+}$ (μmol)	Py (μmol)	n	k
0	1.260	0	0.945	0		
5	0.329	0	0.212	2.147	2.307	0.788
10	0.272	0.019	0.190	2.349	2.261	0.766
15	0.243	0.029	0.176	2.511	2.312	0.758
20	0.240	0.041	0.177	2.741	2.539	0.754
25	0.220	0.050	0.159	2.822	2.531	0.760
30	0.219	0.059	0.157	2.930	2.658	0.762
35	0.203	0.064	0.147	3.038	2.754	0.759
40	0.198	0.068	0.149	3.038	2.715	0.749
45	0.196	0.074	0.149	3.078	2.760	0.746
50	0.178	0.078	0.134	3.119	2.723	0.750
55	0.179	0.083	0.136	3.132	2.736	0.745
60	0.175	0.086	0.131	3.146	2.723	0.749
70	0.170	0.091	0.127	3.173	2.731	0.751
80	0.167	0.098	0.126	3.200	2.735	0.746
90	0.163	0.100	0.123	3.213	2.738	0.749
180	0.141	0.118	0.105	3.308	2.724	0.756
360	0.133	0.126	0.099	3.348	2.725	0.756

Table S15. The quantities of **2**, $[\text{Pd}_6\mathbf{2}_8]^{12+}$, $[\text{PdPy}_4]^{2+}$ and Py and the (n, k) values at each time point for the assembly of $[\text{Pd}_6\mathbf{2}_8]^{12+}$ (4th run)

Time (min)	2 (μmol)	$[\text{Pd}_6\mathbf{2}_8]^{12+}$ (μmol)	$[\text{PdPy}_4]^{2+}$ (μmol)	Py (μmol)	n	k
0	1.152	0	0.854	0		
5	0.345	0	0.193	2.052	2.542	0.818
10	0.263	0.020	0.165	2.174	2.321	0.780
15	0.247	0.030	0.164	2.471	2.631	0.766
20	0.227	0.038	0.152	2.579	2.684	0.763
25	0.221	0.045	0.143	2.633	2.718	0.771
30	0.212	0.052	0.138	2.673	2.716	0.770
35	0.205	0.057	0.135	2.714	2.740	0.767
40	0.195	0.063	0.132	2.754	2.745	0.760
45	0.183	0.067	0.119	2.781	2.705	0.769
50	0.182	0.073	0.120	2.808	2.732	0.766
55	0.182	0.076	0.120	2.822	2.752	0.768
60	0.176	0.078	0.115	2.835	2.734	0.768
70	0.171	0.084	0.110	2.862	2.739	0.777
80	0.161	0.088	0.104	2.903	2.752	0.774
90	0.157	0.091	0.101	2.916	2.735	0.776
180	0.133	0.114	0.088	3.024	2.700	0.763
360	0.130	0.120	0.086	3.051	2.731	0.761

Table S16. The quantities of **2**, $[\text{Pd}_6\mathbf{2}_8]^{12+}$, $[\text{PdPy}_4]^{2+}$ and Py and the (n, k) values at each time point for the assembly of $[\text{Pd}_6\mathbf{2}_8]^{12+}$ (5th run)

Time (min)	2 (μmol)	$[\text{Pd}_6\mathbf{2}_8]^{12+}$ (μmol)	$[\text{PdPy}_4]^{2+}$ (μmol)	Py (μmol)	n	k
0	1.134	0	0.854	0		
5	0.258	0	0.168	1.944	2.220	0.783
10	0.238	0.023	0.166	2.214	2.335	0.771
15	0.222	0.033	0.157	2.336	2.382	0.770
20	0.212	0.044	0.156	2.538	2.599	0.762
25	0.202	0.052	0.150	2.673	2.758	0.760
30	0.194	0.059	0.142	2.700	2.746	0.764
35	0.181	0.065	0.132	2.754	2.756	0.766
40	0.172	0.070	0.127	2.781	2.738	0.763
45	0.165	0.076	0.123	2.822	2.759	0.761
50	0.159	0.079	0.118	2.835	2.738	0.763
55	0.158	0.083	0.118	2.849	2.748	0.762
60	0.156	0.086	0.115	2.862	2.752	0.766
70	0.151	0.090	0.113	2.876	2.719	0.766
80	0.144	0.095	0.107	2.916	2.767	0.769
90	0.146	0.100	0.109	2.916	2.746	0.769
180	0.133	0.117	0.102	2.984	2.708	0.771

Table S17. The quantities of **2**, $[\text{Pd}_6\mathbf{2}_8]^{12+}$, $[\text{PdPy}_4]^{2+}$ and Py and the (n, k) values at each time point for the assembly of $[\text{Pd}_6\mathbf{2}_8]^{12+}$ (6th run)

Time (min)	2 (μmol)	$[\text{Pd}_6\mathbf{2}_8]^{12+}$ (μmol)	$[\text{PdPy}_4]^{2+}$ (μmol)	Py (μmol)	n	k
0	1.323	0	0.992	0		
5	0.352	0	0.232	2.295	2.363	0.783
10	0.323	0.021	0.225	2.592	2.509	0.771
15	0.298	0.034	0.215	2.849	2.699	0.762
20	0.283	0.043	0.203	2.930	2.724	0.764
25	0.266	0.051	0.196	2.957	2.666	0.755
30	0.248	0.059	0.186	3.065	2.731	0.750
35	0.240	0.068	0.179	3.119	2.760	0.753
40	0.225	0.073	0.167	3.173	2.763	0.754
45	0.215	0.078	0.162	3.200	2.743	0.749
50	0.205	0.082	0.155	3.227	2.724	0.747
55	0.197	0.088	0.147	3.267	2.739	0.751
60	0.194	0.090	0.146	3.294	2.777	0.750
70	0.184	0.095	0.136	3.335	2.780	0.754
80	0.178	0.098	0.135	3.348	2.760	0.747
90	0.168	0.102	0.127	3.389	2.775	0.749
180	0.150	0.128	0.113	3.483	2.758	0.750
360	0.145	0.136	0.109	3.510	2.724	0.750

Table S18. The quantities of **2**, $[\text{Pd}_6\mathbf{2}_8]^{12+}$, $[\text{PdPy}_4]^{2+}$ and Py and the (n, k) values at each time point for the assembly of $[\text{Pd}_6\mathbf{2}_8]^{12+}$ (7th run)

Time (min)	2 (μmol)	$[\text{Pd}_6\mathbf{2}_8]^{12+}$ (μmol)	$[\text{PdPy}_4]^{2+}$ (μmol)	Py (μmol)	<i>n</i>	<i>k</i>
0	1.323	0	0.996	0		
5	0.368	0	0.242	2.376	2.488	0.789
10	0.324	0.021	0.229	2.646	2.576	0.771
15	0.286	0.032	0.216	2.876	2.699	0.753
20	0.273	0.042	0.206	2.984	2.765	0.753
25	0.266	0.049	0.197	3.011	2.760	0.760
30	0.248	0.055	0.188	3.078	2.772	0.752
35	0.240	0.062	0.184	3.119	2.779	0.749
40	0.235	0.070	0.180	3.159	2.801	0.749
45	0.221	0.075	0.172	3.200	2.789	0.745
50	0.218	0.079	0.169	3.213	2.782	0.745
55	0.212	0.084	0.165	3.240	2.784	0.743
60	0.206	0.088	0.157	3.254	2.766	0.752
70	0.204	0.095	0.156	3.281	2.791	0.752
80	0.191	0.099	0.144	3.321	2.777	0.758
90	0.187	0.106	0.143	3.335	2.749	0.751
180	0.161	0.129	0.123	3.456	2.772	0.760
360	0.157	0.136	0.121	3.483	2.783	0.750

Table S19. The quantities of **2**, $[\text{Pd}_6\mathbf{2}_8]^{12+}$, $[\text{PdPy}_4]^{2+}$ and Py and the (n, k) values at each time point for the assembly of $[\text{Pd}_6\mathbf{2}_8]^{12+}$ (8th run)

Time (min)	2 (μmol)	$[\text{Pd}_6\mathbf{2}_8]^{12+}$ (μmol)	$[\text{PdPy}_4]^{2+}$ (μmol)	Py (μmol)	<i>n</i>	<i>k</i>
0	1.341	0	0.992	0		
5	0.413	0	0.233	2.349	2.532	0.818
10	0.352	0.014	0.217	2.633	2.620	0.788
15	0.305	0.034	0.196	2.808	2.607	0.775
20	0.283	0.044	0.187	2.970	2.709	0.766
25	0.275	0.055	0.183	3.038	2.741	0.765
30	0.251	0.062	0.172	3.119	2.744	0.754
35	0.241	0.069	0.164	3.159	2.744	0.756
40	0.229	0.075	0.154	3.213	2.757	0.757
45	0.221	0.083	0.149	3.240	2.740	0.758
50	0.212	0.087	0.146	3.281	2.756	0.750
55	0.212	0.093	0.143	3.294	2.752	0.754
60	0.207	0.096	0.139	3.321	2.780	0.758
70	0.198	0.101	0.131	3.348	2.756	0.763
80	0.192	0.108	0.127	3.375	2.746	0.761
90	0.189	0.112	0.128	3.389	2.733	0.750
180	0.164	0.136	0.108	3.510	2.767	0.765
360	0.158	0.142	0.105	3.537	2.750	0.758

Table S20. The quantities of **2**, $[\text{Pd}_6\mathbf{2}_8]^{12+}$, $[\text{PdPy}_4]^{2+}$ and Py and the (n, k) values at each time point for the assembly of $[\text{Pd}_6\mathbf{2}_8]^{12+}$ (9th run)

Time (min)	2 (μmol)	$[\text{Pd}_6\mathbf{2}_8]^{12+}$ (μmol)	$[\text{PdPy}_4]^{2+}$ (μmol)	Py (μmol)	<i>n</i>	<i>k</i>
0	1.350	0	1.006	0		
5	0.383	0	0.227	2.363	2.442	0.805
10	0.332	0.022	0.210	2.687	2.562	0.789
15	0.287	0.034	0.200	2.916	2.655	0.761
20	0.268	0.045	0.191	3.038	2.713	0.755
25	0.244	0.052	0.179	3.132	2.731	0.747
30	0.238	0.062	0.174	3.186	2.755	0.745
35	0.230	0.069	0.168	3.227	2.767	0.746
40	0.225	0.075	0.164	3.254	2.770	0.746
45	0.209	0.081	0.154	3.321	2.793	0.741
50	0.207	0.086	0.151	3.335	2.791	0.744
55	0.202	0.090	0.146	3.348	2.772	0.747
60	0.200	0.098	0.145	3.375	2.796	0.745
70	0.194	0.103	0.140	3.389	2.766	0.748
80	0.186	0.110	0.135	3.429	2.783	0.743
90	0.178	0.111	0.129	3.456	2.788	0.742
180	0.165	0.130	0.117	3.524	2.776	0.745
360	0.150	0.140	0.107	3.578	2.742	0.742

Table S21. The quantities of **2**, $[\text{Pd}_6\mathbf{2}_8]^{12+}$, $[\text{PdPy}_4]^{2+}$ and Py and the (n, k) values at each time point for the assembly of $[\text{Pd}_6\mathbf{2}_8]^{12+}$ (10th run)

Time (min)	2 (μmol)	$[\text{Pd}_6\mathbf{2}_8]^{12+}$ (μmol)	$[\text{PdPy}_4]^{2+}$ (μmol)	Py (μmol)	<i>n</i>	<i>k</i>
0	1.350	0	1.006	0		
5	0.389	0	0.237	2.349	2.444	0.800
10	0.329	0.021	0.210	2.687	2.560	0.786
15	0.302	0.033	0.203	2.903	2.690	0.771
20	0.274	0.042	0.194	3.024	2.723	0.755
25	0.266	0.052	0.189	3.078	2.741	0.756
30	0.255	0.061	0.181	3.146	2.769	0.756
35	0.237	0.069	0.168	3.213	2.774	0.755
40	0.228	0.073	0.160	3.240	2.763	0.757
45	0.221	0.081	0.157	3.281	2.780	0.754
50	0.212	0.085	0.150	3.308	2.771	0.755
55	0.203	0.091	0.143	3.348	2.779	0.756
60	0.204	0.095	0.144	3.348	2.768	0.757
70	0.189	0.102	0.132	3.402	2.767	0.758
80	0.184	0.107	0.128	3.429	2.773	0.760
90	0.181	0.111	0.128	3.443	2.769	0.752
180	0.166	0.133	0.116	3.524	2.761	0.761
360	0.150	0.145	0.106	3.591	2.780	0.759

n-k Analysis for the assembly of the $[Pd_6L_8]^{12+}$ ($L = 1$ or 2) capsules

Ten experiments were conducted for investigating the assembly process of each $[Pd_6L_8]^{12+}$ capsule ($L = 1$ or 2). The (n, k) plots for the assembly of $[Pd_6\mathbf{1}_8]^{12+}$ and $[Pd_6\mathbf{2}_8]^{12+}$ are shown in Supplementary Figures S2a-j and S3a-j, respectively. These results unambiguously confirm the high reproducibility of the measurements. The average (n, k) values from 20 to 360 min for $[Pd_6\mathbf{1}_8]^{12+}$ and $[Pd_6\mathbf{2}_8]^{12+}$ are shown in Supplementary Figures S2k and S3k, respectively, indicating that the steps from $[Pd_6\mathbf{1}_8Py]^{12+}$ and $[Pd_6\mathbf{2}_8Py_2]^{12+}$ are the rate-determining steps.

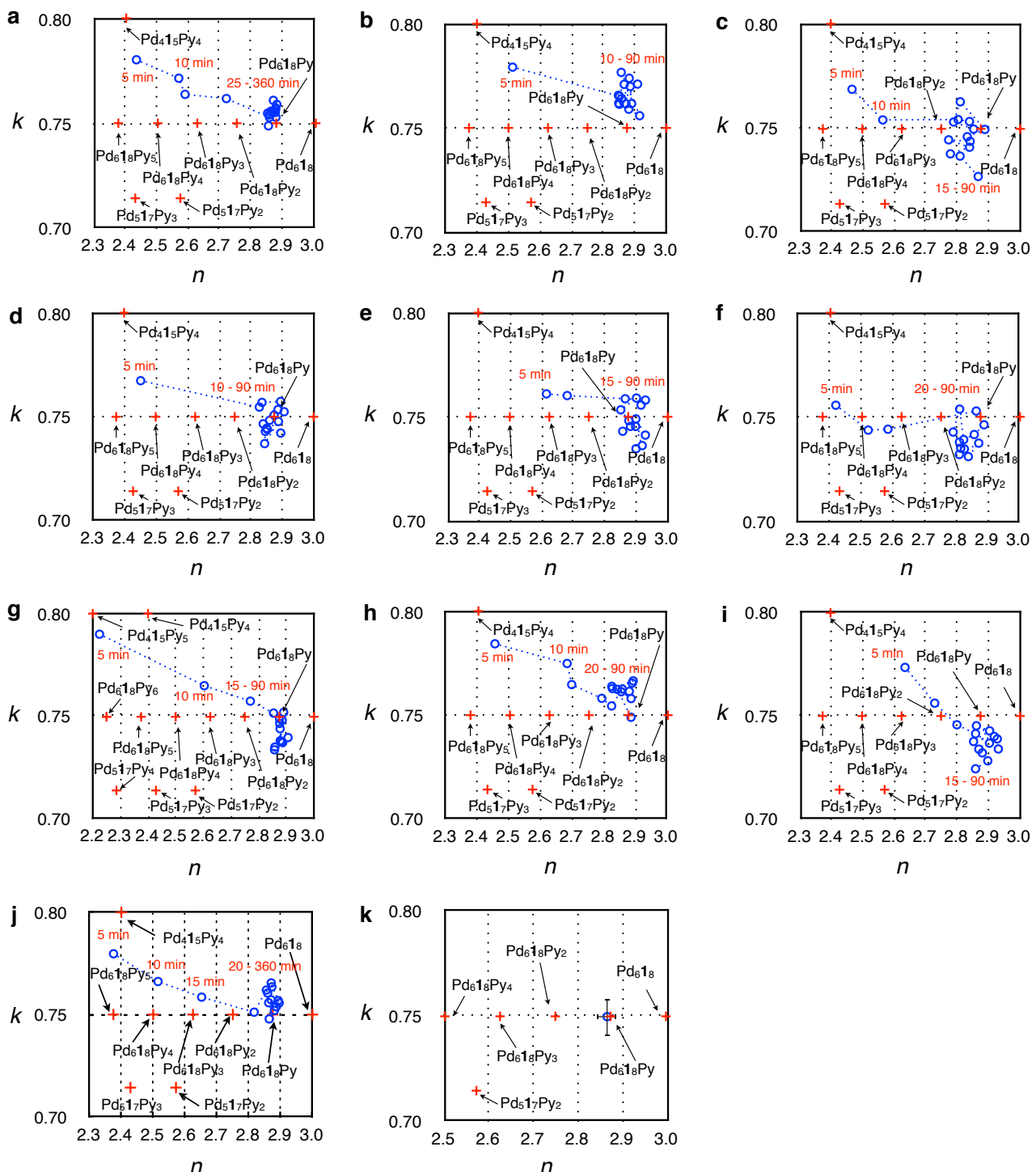


Fig. S2 n - k Plots for the self-assembly of $[Pd_6\mathbf{1}_8]^{12+}$. a – j) n - k plots of ten experiments for the assembly of $[Pd_6\mathbf{1}_8]^{12+}$. k) A plot of the average (n, k) value with standard deviations from 20 to 360 min for the ten experiments (a – j).

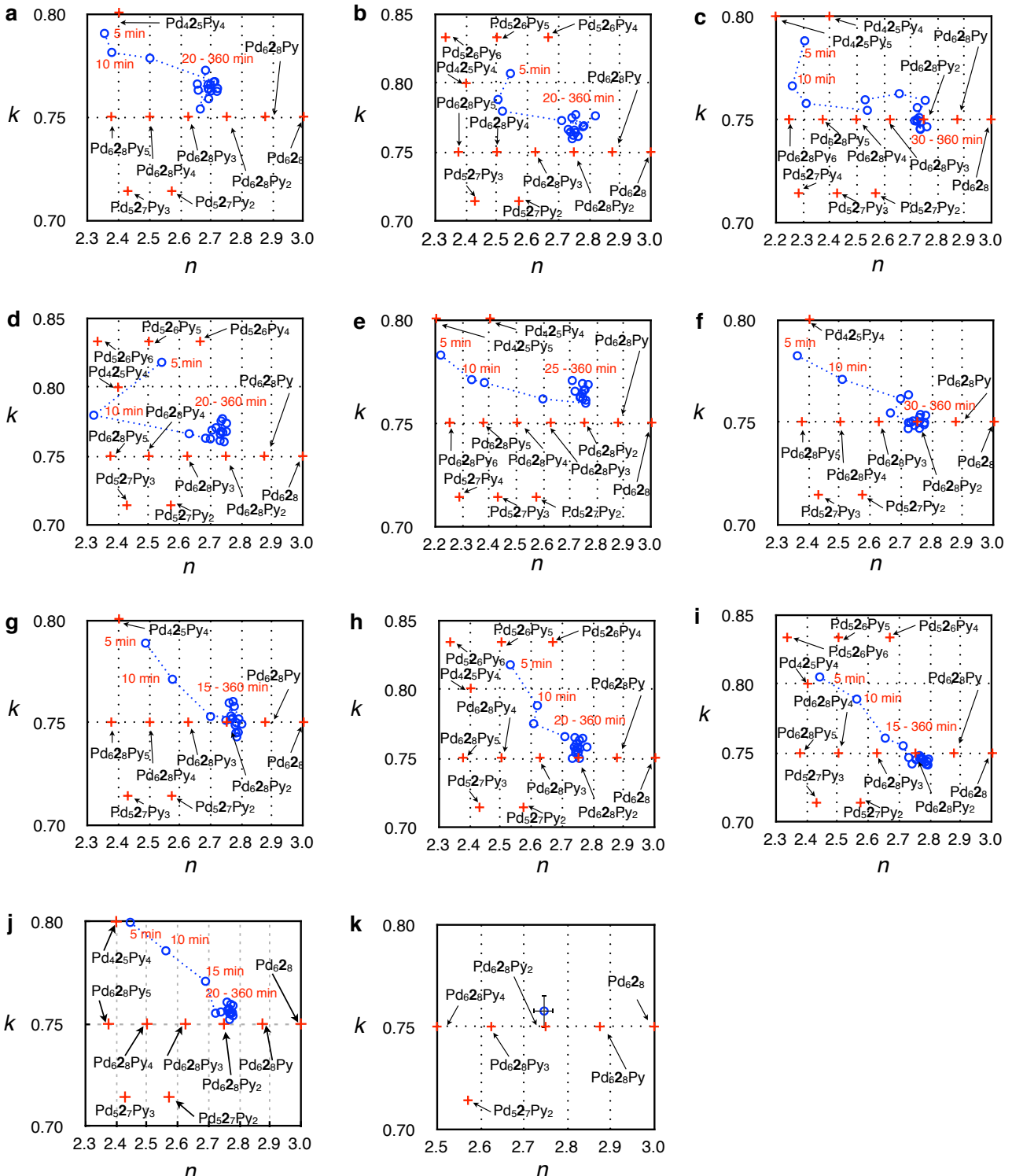


Fig. S3 n - k Plots for the self-assembly of the $[Pd_628]^{12+}$ capsule. a – j) n - k plots of ten experiments for the assembly of $[Pd_628]^{12+}$. k) A plot of the average (n , k) value with standard deviations from 20 to 360 min for the ten experiments (a – j).

ESI-TOF mass study for the assembly of $[Pd_6L_8]^{12+}$ ($L = 1$ or 2)

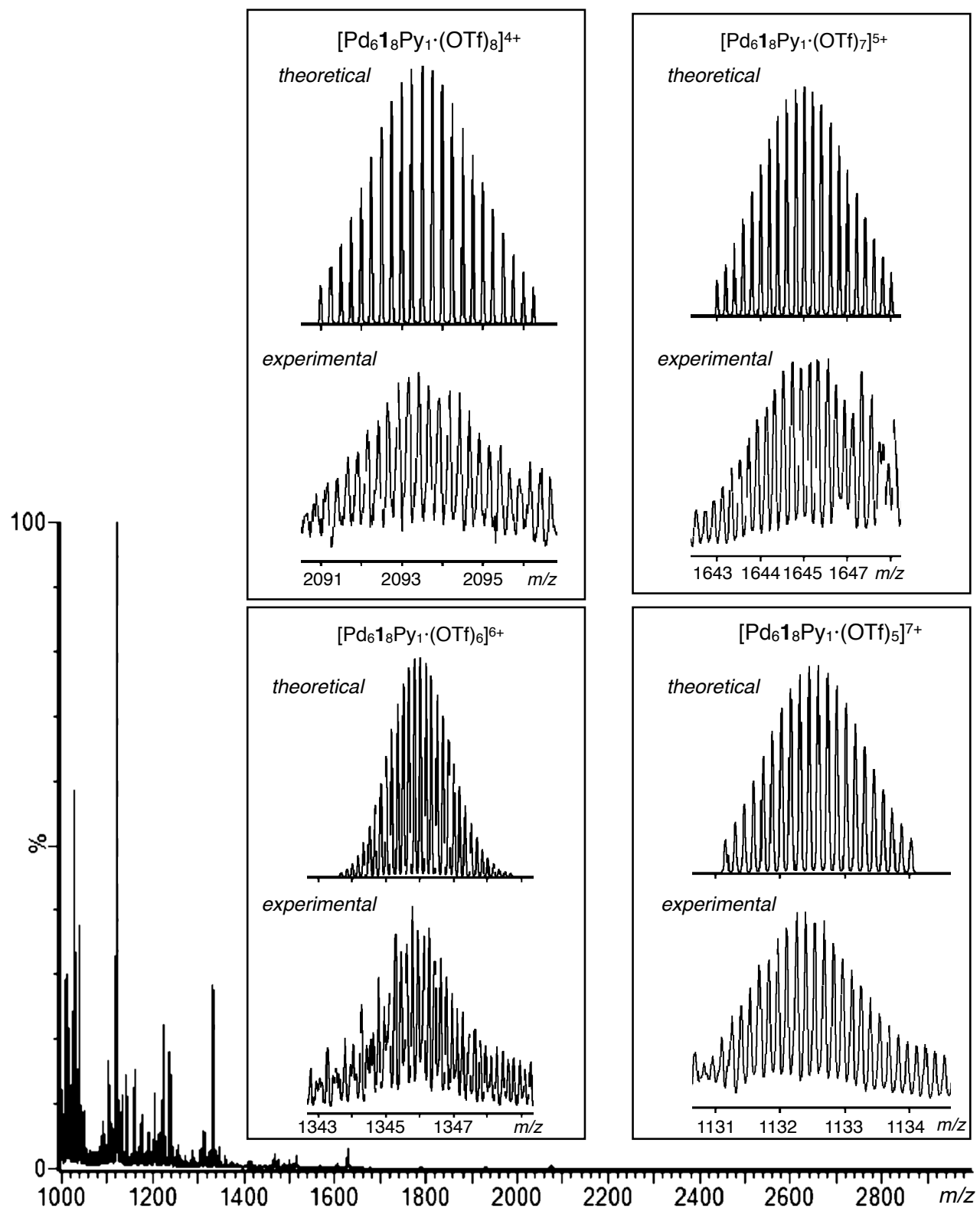


Fig. S4 ESI-TOF mass spectrum for the assembly of the $[Pd_6\mathbf{1}_8]^{12+}$ capsule measured after 20 min.

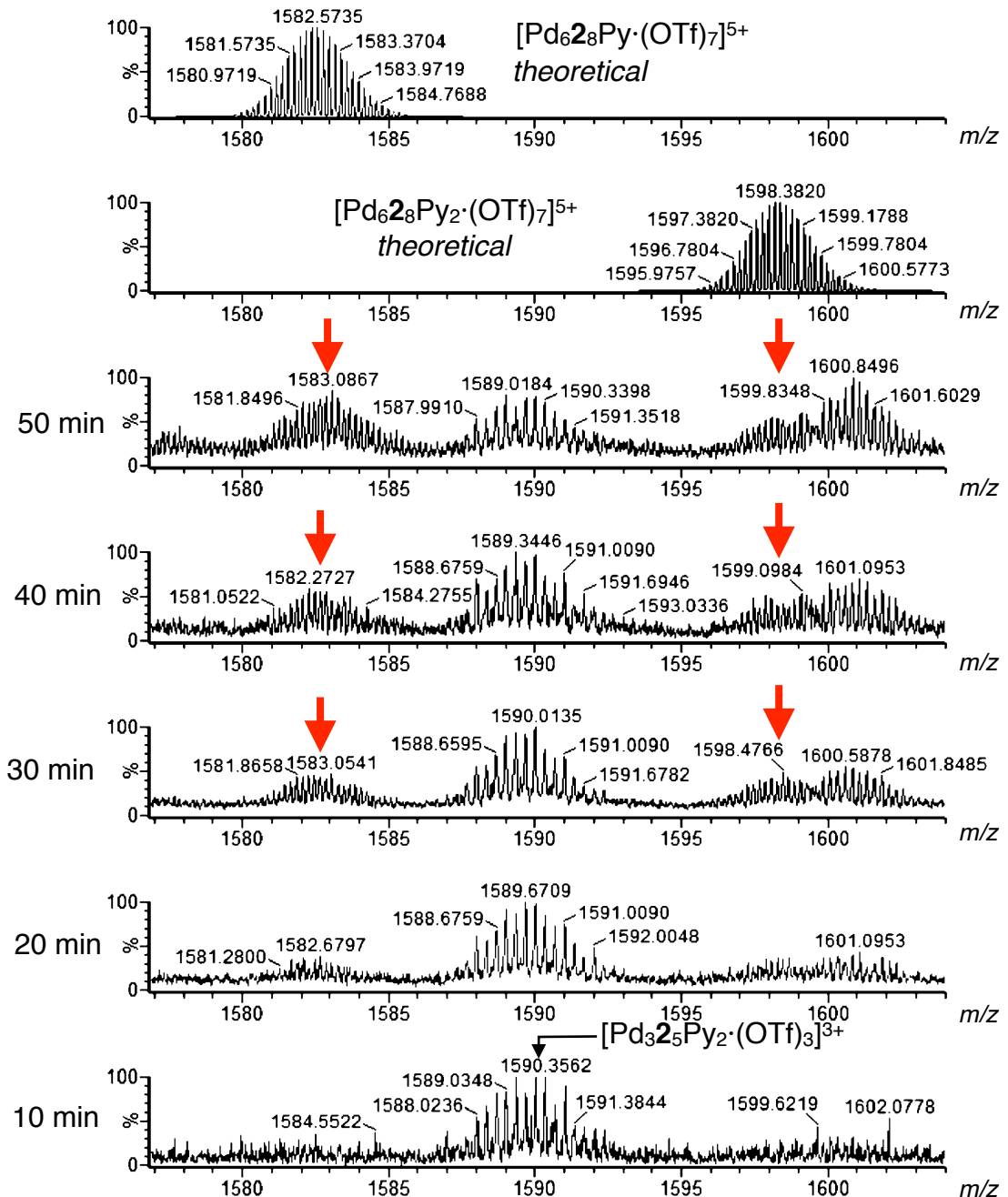


Fig. S5 Time-course ESI-TOF mass spectra for the assembly of the $[Pd_6L_8]^{12+}$ capsule ($m/z = 1577 - 1604$).

The structural isomers of $[\text{Pd}_6\text{L}_8\text{Py}_2]^{12+}$

$[\text{Pd}_6\text{L}_8\text{Py}_2]^{12+}$ has nine structural isomers in which the position of the two Py's coordinating to Pd^{2+} centre(s) is different. The nine structures are shown in Fig. S6.

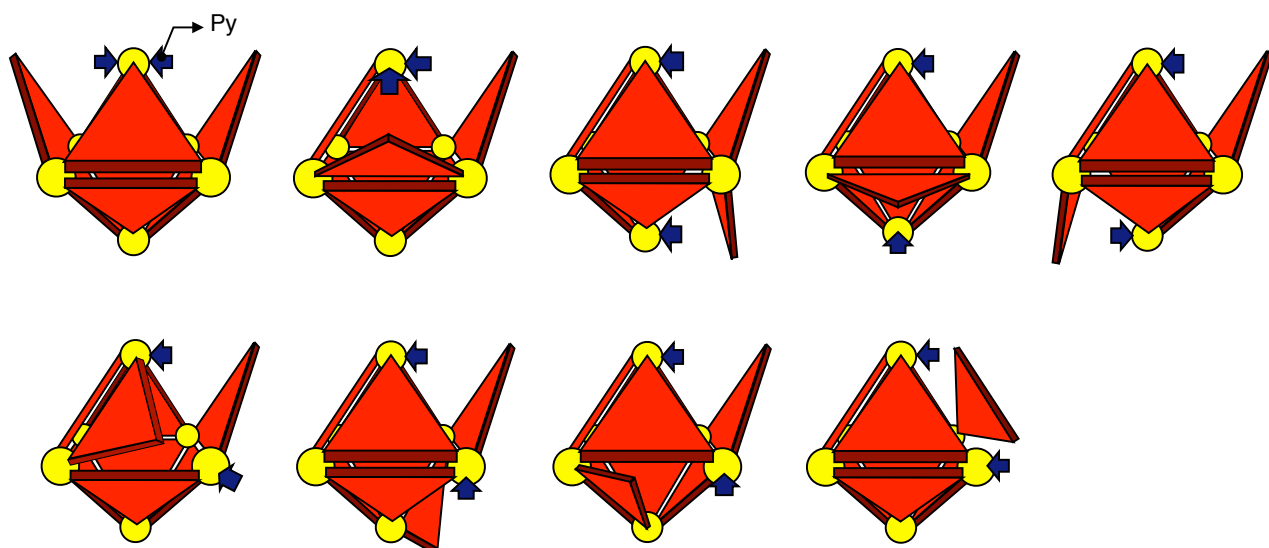


Fig. S6. Schematic representation of the structural isomers of $[\text{Pd}_6\text{L}_8\text{Py}_2]^{12+}$.

Molecular Mechanics investigation of the strain energy of the intermediates in the last step of the self-assembly process

The present study indicates that the energy barrier of the last step of the assembly of $[\text{Pd}_6\mathbf{1}_8]^{12+}$, from $[\text{Pd}_6\mathbf{1}_8\text{Py}_1]^{12+}$ to $[\text{Pd}_6\mathbf{1}_8]^{12+}$, is higher than that for the assembly of $[\text{Pd}_6\mathbf{2}_8]^{12+}$. This would be due to the higher strain energy of the transition state (or five-coordinate intermediates) in the last step of the assembly for $[\text{Pd}_6\mathbf{1}_8]^{12+}$. To support this rationale, we conducted *MM* calculations (Material Studio Ver. 4.0, Universal Force field, Accelrys Software Inc.) of the ground state and the intermediate of the last step, in which one Pd^{2+} centre has a square-pyramidal coordination geometry, for $[\text{Pd}_6\mathbf{1}_8\text{Py}_1]^{12+}$ and $[\text{Pd}_6\mathbf{2}'_8\text{Py}_1]^{12+}$ ($\mathbf{2}'$ is the panel molecule in which three deuterium atoms of $\mathbf{2}$ is replaced with hydrogen atoms) and their valence energies were compared. In addition, to evaluate the effect of the changes in the coordination geometry to the valence energies, *MM* calculations of the mononuclear complexes, a square-planar $[\text{PdPy}_4]^{2+}$ and a square-pyramidal $[\text{PdPy}_5]^{2+}$, were carried out. All the structures are shown in Fig. S7 and the valence energies of the structures are listed in Table S3. It was found that the energy difference between the ground state and the intermediate for $[\text{Pd}_6\mathbf{1}_8\text{Py}_1]^{12+}$ is larger than that for $[\text{Pd}_6\mathbf{2}'_8\text{Py}_1]^{12+}$, while the energy differences for $[\text{Pd}_6\mathbf{2}'_8\text{Py}_1]^{12+}$ and for the mononuclear Pd^{2+} complexes are similar to each other. These results suggest that the higher valence energy for $[\text{Pd}_6\mathbf{1}_8\text{Py}_1]^{12+}$ would arise from the steric effect of the methyl groups in $\mathbf{1}$.

Table S3. Valence energies of the ground state and the intermediate for $[Pd_6L_8Py_1]^{12+}$ and $[Pd_6L_8Py_2]^{12+}$ and a square-planar $[PdPy_4]^{2+}$ with a free Py and a square-pyramidal $[PdPy_5]^{2+}$

	Valence energy (kcal/mol)		
	$[Pd_6L_8Py]^{12+}$	$[Pd_6L'_8Py]^{12+}$	$[PdPy_5]^{2+}$
Ground state (square-planar)	767.675	705.834	5.471
Intermediate (square-pyramidal)	799.624	719.269	18.581
Difference	31.949	13.435	13.110

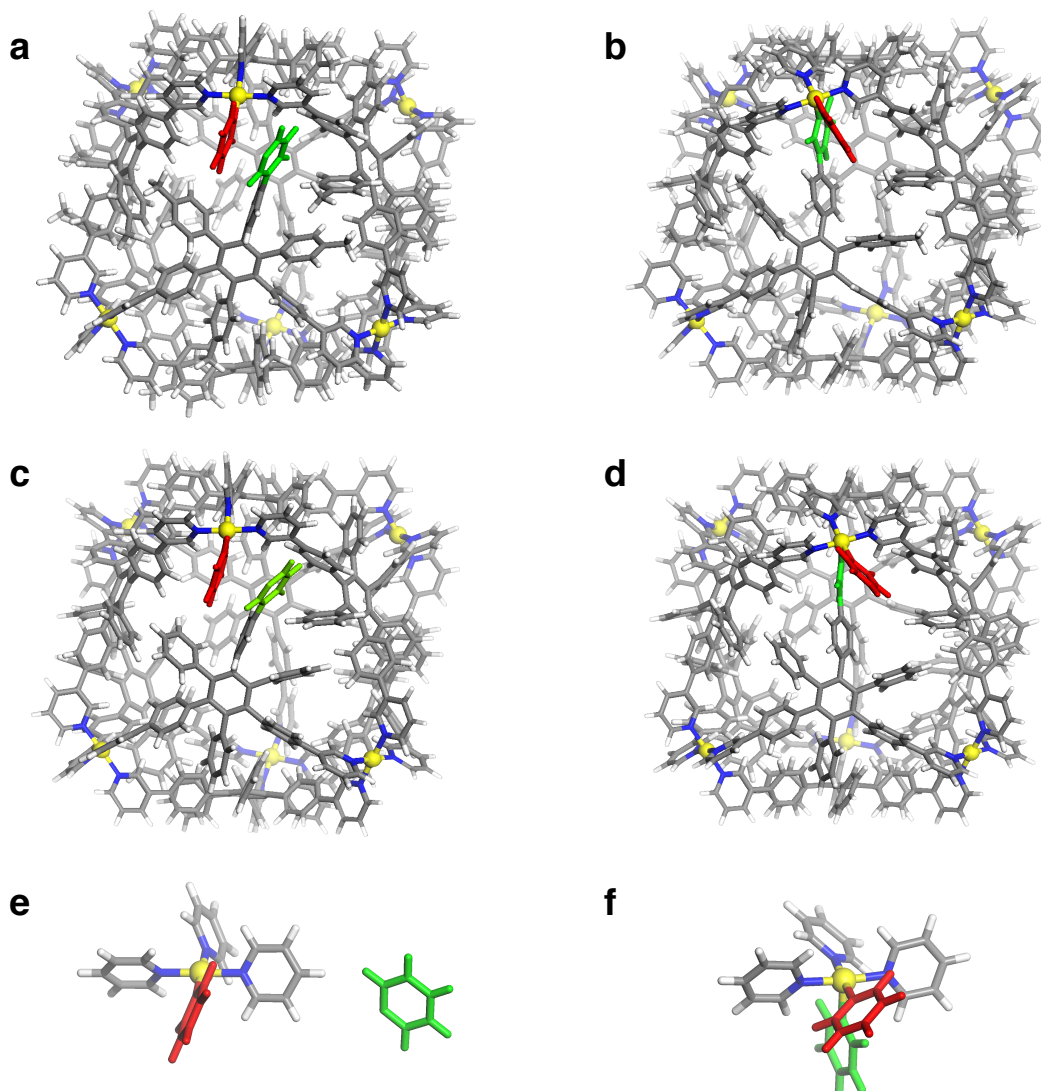


Fig. S7. The optimized structures of (a) the ground state $[Pd_6L_8Py_1]^{12+}$, (b) the intermediate $[Pd_6L_8Py_1]^{12+}$, (c) the ground state $[Pd_6L'_8Py_1]^{12+}$, (d) the intermediate $[Pd_6L'_8Py_1]^{12+}$, (e) $[PdPy_4]^{2+}$ with a Py and (f) $[PdPy_5]^{2+}$. Colour labels: grey: C, white: H, blue: N, yellow: Pd, green: free pyridine ring in the panel molecule, red: Py in the $[Pd_6L_8Py_1]^{12+}$ structures.

References

- [1] R. Rathore and C. L. Burns, *Org. Synth.*, 2005, **82**, 30.
- [2] T. Kojima and S. Hiraoka, *Org. Lett.*, 2014, **16**, 1024.